

28 **Abstract**

29 **Objective:** Pulmonary arterial hypertension (PAH) is characterized by exercise intolerance.
30 Muscle blood flow may be reduced during exercise in PAH; however, this has not been directly
31 measured. Therefore, we investigated blood flow during exercise in a rat model of monocrotaline
32 (MCT)-induced PH. **Methods:** Male Sprague-Dawley rats (~200g) were injected with 60mg/kg
33 MCT (MCT, n=23) and vehicle control (saline; CON, n=16). VO_{2max} and voluntary running
34 were measured prior to PH induction. Right ventricle (RV) morphology and function was
35 assessed via echocardiography and invasive hemodynamic measures. Treadmill running at 50%
36 VO_{2max} was performed by a subgroup of rats (MCT, n=8; CON, n=7). Injection of fluorescent
37 microspheres determined muscle blood flow via photo spectroscopy. **Results:** MCT
38 demonstrated a severe phenotype via RV hypertrophy (Fulton Index, 0.61 vs. 0.31; $p<0.001$),
39 high RV systolic pressure (51.5 vs. 22.4 mmHg; $p<0.001$) and lower VO_{2max} (53.2 vs. 71.8
40 $mL \cdot min^{-1} \cdot kg^{-1}$; $p<0.0001$) compared to CON. Two-way ANOVA revealed exercising skeletal
41 muscle blood flow relative to power output was reduced in MCT compared to CON ($p<0.001$)
42 and plasma lactate was increased in MCT (10.8 vs. 4.5 mmol/L; $p=0.002$). Significant
43 relationships between skeletal blood flow and blood lactate during exercise was observed for
44 individual muscles ($r = -0.58$ to -0.74 ; $p<0.05$). No differences in capillarization were identified.
45 **Conclusion:** Skeletal muscle blood flow is significantly reduced in experimental PH. Reduced
46 blood flow during exercise may be, at least in part, consequent to reduced exercise intensity in
47 PH. This adds further evidence of peripheral muscle dysfunction and exercise intolerance in
48 PAH.

49 Key words: PAH, Skeletal Muscle, Monocrotaline

50

51

52 **Introduction**

53 Pulmonary arterial hypertension (PAH) is a devastating progressive disorder in which
54 thrombosis, proliferation, inflammation and remodeling of the lung vasculature leads to a
55 narrowing of pulmonary arteries and subsequent right ventricular (RV) pressure overload,
56 dilation, and ultimately failure (1). Significant strides have been made in understanding complex
57 PAH pathophysiology; however, patient prognosis remains poor (2) and a cure remains elusive.
58 Importantly, even with optimal pharmacological treatment, PAH patients still suffer from
59 reduced quality of life and a profound exercise intolerance (3-5). This dysfunction is
60 characterized by lower maximal aerobic capacity (6, 7), compromised pulmonary function (8, 9),
61 reduced muscle strength and power (10-13) and early-onset dyspnea and fatigue (7, 14). As such,
62 interest in the connection between PAH pathophysiology and exercise limitation has increased in
63 recent years, revealing complex central and peripheral abnormalities as a consequence of the
64 disease (15).

65 Previous work has shown that compromised RV function, including an inability to
66 maintain stroke volume and subsequent left ventricular (LV) filling limits cardiac output at the
67 onset of exercise in PAH (16). Additionally, it has been observed that patients display
68 chronotropic incompetence (17), RV/LV dyssynchrony (18-20) and reduced myocardial
69 contractility (21). Additionally, increased pulmonary vascular resistance reduces RV cardiac
70 output (Waxman et al., 2012), and compromised respiratory dynamics (22-24) have been
71 implicated as contributors to exercise intolerance in the disease. Importantly, abnormalities
72 specific to skeletal muscle have also been shown to limit exercise performance in both PAH
73 patients and animal models. Upper and lower body muscle strength and endurance are reduced

74 (11, 12, 25-27), and these limitations have been directly associated with functional performance.
75 In addition, skeletal muscle mitochondrial dysfunction and reliance on non-oxidative metabolism
76 have been identified both in patient studies (12, 28) and supported by our group and others in
77 animal models (29, 30). Finally, several investigators have shown that reduced capillarity and
78 microcirculation in skeletal muscle blunts exercise capacity (13, 27, 31) indicating
79 morphological changes that develop as a consequence of disease.

80 While it is clear that multiple factors play a role in limiting exercise in PAH, it is still
81 uncertain whether exercise limitations in PAH are due to reduced blood flow to skeletal muscle.
82 Adequate blood flow is essential to the maintenance of exercise, however, to our knowledge,
83 skeletal muscle blood flow has not been *directly* measured in PAH. Indeed, interrogating the role
84 of oxygen delivery to exercising muscle during exercise has recently been identified as an
85 important knowledge gap that requires further investigation (15). Therefore, the purpose of this
86 study was to characterize directly-measured blood flow in an animal model of PH. We
87 hypothesized that in rats with experimental PH, skeletal muscle blood flow would be reduced at
88 both rest and during moderate intensity exercise.

89 **Materials and Methods**

90 **Ethical Approval**

91 The experimental protocol was approved by the Institutional Animal Care and Use Committee of
92 Indiana University, which is in compliance with National Institutes of Health guidelines.

93 **Animals**

94 Male Sprague–Dawley rats (~200 g; Charles River Chicago, Illinois, USA) were used in this
95 study. Only male rats were studied because the model employed (i.e., monocrotaline (MCT)
96 injection) does not reliably produce a PH phenotype in the female rat (32), likely due to differing

97 metabolism of MCT in the liver (33, 34). All animals were housed in pairs in the Indiana
98 University animal facility and fed standard rat chow and water ad libitum. The rats were
99 maintained at an ambient temperature of 21–24°C with a 12 h–12 h dark–light cycle.

100 **PH Induction and Experimental Groups**

101 PH was induced via a single MCT injection (60 mg/kg, s.q. in sterile PBS, Sigma Aldrich) that
102 reliably produces a severe PAH phenotype at ~4 wk post injection (Hessel et al., 2006). Control
103 animals (CON) received vehicle (saline, s.q.). Animals were then grouped as MCT (n=23) and
104 CON (n=16) for phenotyping, with sub-groups from those (MCT, n=8 and CON, n=7) included
105 in blood flow analysis. The timeline for PH induction and subsequent measures are described in
106 Figure 1.

107 **Treadmill Familiarization and Aerobic Capacity Testing**

108 As running is a skilled activity for rats, familiarization to the rodent motorized treadmill
109 was performed for 4 d before exercise testing. The familiarization protocol involved 4 x 5 min
110 runs that gradually increased treadmill speed (8-12 m/min) and incline (0 to 15 deg). These
111 inclines and speeds are similar to those experienced during maximal aerobic testing.
112 Familiarization runs were limited to minimize chronic training effects before baseline testing. A
113 mild electric stimulus at the back of the treadmill chamber promoted the learning of running
114 behavior, and the ability of the rat to run successfully was documented through this
115 familiarization period. ‘Cueing’, including the use of verbal encouragement, treadmill lane taps
116 and group-running were used to promote consistent running toward the front of the treadmill
117 belt. If a rat contacted the stimulus three consecutive times without the ability to recover to the
118 front of the treadmill belt, the familiarization session was terminated.

Exercising Blood Flow in Pulmonary Hypertension

119 VO_2max was measured using an indirect calorimetry system paired with the motorized
120 rodent treadmill (Columbus Instruments, Columbus, OH). Gas analyzer calibrations were
121 conducted before testing using standardized gas mixtures (20.97 - 20.98% O_2 , 0.044% CO_2
122 measured to within 0.01% of the target concentration - Praxair, Indianapolis, IN, USA). Baseline
123 VO_2 was monitored for 3-5 minutes until stabilization, and this was recorded as “resting VO_2 ”.
124 An incremental treadmill running protocol (modified from Kemi et al. (35)) was then
125 administered, using 3 min stages as follows: 8 m/min at 5 deg (warm up), 8 m/min at 15 deg, 9.8
126 m/min at 15 deg, 11.6 m/min at 15 deg, etc., with the speed continuing to increase by 1.8 m/min
127 every 3 min until test completion. Flow rate to the chamber was 4.34 l/min, and VO_2 was
128 measured at 20 s intervals throughout. The test was terminated when VO_2 plateaued despite
129 increasing workload, or if the rat was unable to maintain running after three consecutive
130 electrical stimuli without recovery to the front of the treadmill belt. The highest VO_2 measured in
131 the minute following test completion was recorded as VO_2max and expressed relative to body
132 weight ($\text{mL}\cdot\text{min}^{-1}\cdot\text{g}^{-1}$). The final VO_2max test was used to determine relative exercise intensities
133 for blood flow analysis.

134 **Voluntary Wheel Running**

135 For measurement of volitional wheel running activity, rats were familiarized for 24 h in a
136 cage equipped with a computer-monitored running wheel (Lafayette Instruments, Model 80850S
137 Scurry Rat Activity Wheel), with wheel revolutions recorded by 86115 Scurry Sensor/Counter,
138 86130 Interface and 86165 Scurry Software, connected to a computer interface for complete data
139 collection (3 s sample rate), analysis and charting. Voluntary running distance (in m) was
140 subsequently measured over a single 12 h dark cycle.

141 **Echocardiography**

142 Echocardiography was performed one day before blood flow testing. Rats were
143 anesthetized with 5% isoflurane in an induction box and then placed on the heated platform with
144 a nose cone and maintained at 1-2%. The hair was clipped over the chest and fine hair removed
145 using a depilatory cream. The skin was cleaned with wet gauze squares. Ultrasonic gel was placed
146 over the chest for the echo procedure and an ultrasonic probe of approximately 6 cm by 8 cm
147 was placed in contact with the gel. Two-dimensional short axis and long axis images were
148 acquired by using a high-resolution ultrasound system as previously described (36). Upon
149 determination of all echocardiographic end points, rats were recovered from anesthesia and
150 placed into a heated cage to recover. All images were obtained by a blinded sonographer.

151 **Surgical Preparation and Blood Flow Measurement**

152 Blood flow to skeletal muscle was measured via injection of fluorescent microspheres as
153 initially described by Ishise et al. (37) and Glenny et al. (38) during and after moderate intensity
154 running (50% VO_2 max) for MCT and CON. Rats were anesthetized by inhaled isoflurane and
155 then orotracheally intubated with a catheter (14 ga) and mechanically ventilated using a tidal
156 volume of 6 mL/kg and a rate of 65-70 breaths/min. End expiratory pressures were at 3-4 cmH₂O
157 by a water overflow on the expiratory limb of the ventilator. The rats were placed on a servo-
158 controlled heated tray that maintains animal temperature at 37° C. Animals were shaved (total
159 abdominal, thoracic surfaces), and the skin cleansed with Betadine and ETOH. The animal was
160 fixed to the operating table with adhesive tape and covered with sterile drape with a hole
161 allowing access to the surgical area. The animal was administered carprofen (5 mg/kg; 0.1-0.5
162 mL, s.q.) before surgery. The right carotid artery and caudal (tail) artery were cannulated via
163 cutdowns through small skin incisions. Arterial and airway pressures were measured
164 continuously. Normal saline boluses (10 mL/kg) were given at the beginning of the procedure to

Exercising Blood Flow in Pulmonary Hypertension

165 replace blood loss from surgery, blood sampling, and ongoing insensible losses during surgery.
166 After placement, tubing was tunneled subcutaneously between the scapulae, and tied in with
167 approx. 25 cm of external line access for microsphere delivery and reference blood sampling in
168 carotid and caudal lines. Incisions were closed using silk suture for muscle layers and
169 monofilament suture for skin. Following surgery, animals were placed back in the cage for
170 recovery (minimum >1 h) in preparation for exercising and resting blood flow measures. To
171 mitigate the potential anticipatory response demonstrated in trained rats (39) exercise measures
172 were carried out prior to those at rest. In both conditions, fluorescent microspheres were prepared
173 for infusion by sonicating for >5 min and vigorously vortexing for >1 min. The caudal artery line
174 was flushed with 0.5 mL saline to encourage effective bleed-back of reference blood. Running
175 was initiated at moderate intensity as determined by calculating 50% VO_2max as described.
176 After 3 min of running at the predetermined intensity to establish a steady-state, fluorescent
177 microspheres (n=approx. 400,000, Red 580/620, Molecular Probes) were injected over 10 s into
178 the carotid cannula. The line was subsequently flushed with 0.5 mL heparinized saline to ensure
179 all spheres were successfully injected. 10 s prior to microsphere infusion, collection of a
180 reference blood sample from the caudal cannula was begun using a motorized syringe
181 withdrawal pump (Kent Scientific, CT, USA). Blood was collected for 60 s at a constant rate of 1
182 mL/min. Following exercise measures, the rat rested for 1-hour before determination of resting
183 blood flow. At this time, a second microsphere infusion of a different color (n=approx. 400,000,
184 Yellow-Green, 500/545, Molecular Probes) was performed in the same manner.

185 **Plasma Lactate**

186 Plasma lactate was measured using a small sample of arterial blood from the caudal line
187 used for reference blood sampling. Approximately 10 μL of blood was withdrawn after the

188 reference blood sample and immediately analyzed using a portable lactate analyzer (Lactate Pro,
189 Sports Resource Group, USA), previously used to measure blood lactate in exercising rats (40,
190 41).

191 **Invasive Hemodynamics**

192 Immediately after resting blood flow and lactate measures, rats were anaesthetized by
193 inhalation of isoflurane-O₂ mixture (5%), orotracheally intubated and mechanically ventilated
194 under isoflurane maintenance (2%). The left carotid artery was cannulated with PE-50 tubing
195 and the right internal jugular vein with a 2F Millar catheter (Millar Instruments, Houston, TX,
196 USA). Surgery was performed on a servo-controlled heated tray that maintained animal
197 temperature at 37°C. Recordings of pulmonary and systemic pressures were achieved within 30
198 minutes following transfer out of the treadmill chamber. Right ventricular systolic pressure
199 (RVSP) and mean arterial pressure (MAP) were assessed in room air and recorded
200 simultaneously.

201 **Tissue Processing**

202 Immediately after hemodynamic measurements, rats were euthanized under anesthesia
203 (5% isoflurane-O₂ mixture) via exsanguination and bilateral pneumonectomy as a secondary
204 means of euthanasia which also allowed for immediate access to the diaphragm and heart
205 muscles. Right ventricular hypertrophy was assessed by measuring the Fulton index [weight of
206 the RV divided by weight of the left ventricle plus septum (S); $RV/(LV + S)$]. Sections of RV
207 and muscle [(biceps femoris (BF), semitendinosus (ST), extensor digitorum longus (EDL),
208 tibialis anterior (TA), gastrocnemius (GA), soleus (SL), rectus femoris (RF), vastus lateralis
209 (VL)] were then snap-frozen in liquid N₂ then stored at -80° C for later biochemical analysis and
210 imaging. Samples from the same muscle groups were collected from the contralateral leg for

Exercising Blood Flow in Pulmonary Hypertension

211 blood flow quantification. Muscles were weighed and placed in 5% ethanolic KOH for 48 h for
212 tissue degradation. Samples were regularly vortexed to ensure full degradation. Reference blood
213 samples collected during exercise and at rest were processed in the same fashion. After
214 degradation, samples were reverse-filtered through 5 μm polyamide mesh filters (Sterlitech, WA,
215 USA). Each filter was carefully placed into a 1.5 mL microcentrifuge tube (Thermo Fisher, MA,
216 USA) and 1 mL of cellosolve acetate (2-ethoxyethyl acetate, 98%, Sigma Aldrich) was added to
217 each of the tubes to degrade microspheres and expose the fluorescence. At 1 h tubes were
218 vortexed to ensure maximum exposure to cellosolve acetate. This was repeated at 2 h. 100 μL
219 samples from each tube were then loaded in duplicate into a 96 well plate in preparation for
220 spectroscopic analysis.

221 **Blood flow quantification**

222 All fluorescence measurements were made using a SpectraMax i3x microplate reader
223 (Molecular Devices, CA). Red fluorescence (representing exercising flow) was measured at an
224 excitation of 580 nm and an emission of 620 nm, and yellow-green fluorescence (representing
225 resting flow) was measured at an excitation of 500 nm and an emission of 545 nm. Tissue blood
226 flow was calculated using equation 1 (38, 42):

227 | 1. $Flow \left(\frac{\text{mL}}{\text{min}} \right) = \frac{(\text{fluorescence of sample}) \times (\text{reference line withdrawal rate})}{(\text{fluorescence of reference blood})}$

228 Blood flow units are calculated and presented as $\text{ml} \cdot \text{min}^{-1} \cdot 100 \text{ g}^{-1}$ of tissue (at rest) by dividing
229 the calculated flow by the recorded muscle sample weight at time of harvest. Exercising blood
230 flows are presented as relative to power output at time of microsphere infusion ($\text{ml} \cdot \text{min}^{-1} \cdot 100$
231 g^{-1}/W). Power was calculated using equation 2:

232 2. *Power (W)* =

233
$$\text{body mass (kg)} \times 9.801 \frac{N}{kg} \times \text{treadmill speed} \left(\frac{m}{min} \right) \times \frac{1 min}{60 s} \times \sin(15^\circ)$$

234 Bilateral kidney flow was used as a measure of adequate microsphere mixing and subsequent
235 uniform systemic blood flow *in vivo*, with a discrepancy of >20% in flow across right and left
236 kidneys resulting in that animal being disregarded from blood flow analysis.

237 **Capillarization**

238 To determine if muscle capillarization differed between MCT and CON rats,
239 immunofluorescent staining was performed with frozen sections from two different sampled
240 muscles, the predominantly type I (slow twitch) soleus, and the predominantly type II (fast
241 twitch) extensor digitorum longus (EDL). The midsection of frozen muscles was cut, embedded
242 in OCT (Fisher Scientific, USA) and frozen at -80 °C until subsequent tissue sectioning. Muscles
243 were sectioned at 8 µm using a cryostat (Reichert-Jung Frigocut 2800) at -20 °C and mounted on
244 Superfrost Plus Microscope Slides (Fisher Scientific, USA). Slides were submerged in 2%
245 paraformaldehyde for 10 min. They were subsequently air-dried and stored at -80 °C in
246 preparation for staining. After three washes in phosphor-buffered saline with Tween (PBS-T,
247 Fisher Scientific, USA) sections were incubated for 48hrs at 4° C with an antibody cocktail
248 containing 1:500 dilution Wheat Germ Agglutinin (W6748 WGA-oregon green 488 conjugate
249 5mg, Thermo Fisher, USA), 1:75 dilution lectin (isolectin GS-IB4 alexaFluor 594 conjugate,
250 Thermo Fisher, USA) in Tris Buffered Saline (TBS) vehicle (Thermo Fisher, USA). Negative
251 controls were processed similarly, with antibodies replaced by incubation in TBS only. Slides
252 were washed three times in PBS-T, after which coverslips containing DAPI ProLong Gold
253 (Fisher Scientific, USA) for nuclei staining were mounted to slides and fixed using Biotium
254 Coverslip Sealant (Biotium, CA, USA). Tissue sections were imaged using a Nikon Eclipse Ti2

255 inverted fluorescence microscope (NY, USA). Three different fields were imaged in each tissue
256 section (9 per muscle sample). Green, red and blue images were taken at their optimal exposure
257 times and exported to ImageJ (NIH, USA). A technician blinded to group assignments counted
258 myocyte and capillary numbers in each field, and calculated capillary to fiber ratio for all muscle
259 sections.

260 **Statistical analysis**

261 Statistical analyses were performed using GraphPad Prism 7.0 (San Diego, CA, USA).
262 Data are presented as means \pm SEM. Differences at α level of 0.05 ($p < 0.05$) were considered
263 statistically significant. In addition to analyzing blood flow measured within each harvested
264 skeletal muscle, a 'compiled blood flow' variable was also created by averaging resting flow and
265 separate exercising flow in individual muscles for each rat. Parametric T-testing for comparison
266 between MCT and CON groups was performed for the following measurements:
267 Echocardiography (stroke volume, cardiac output, cardiac index, RV thickness, PAT, TPRi) RV
268 hypertrophy (Fulton Index, RV weight) RVSP, RVSP/MAP, body weight and aerobic capacity
269 ($VO_2\max$) and exercise behavior (voluntary wheel running) and capillarization. Two-way
270 analysis of variance (ANOVA) by group assignment and muscle was used to interrogate
271 differences in blood flow. Pearson product correlations were used to determine relationships
272 between blood flow and metabolic/disease measures.

273 **Results**

274 **PH Phenotype**

275 Four weeks after MCT injection, rats showed a PH phenotype (Fig. 2 A-C) as expected,
276 demonstrated by an increased RV weight (0.22 ± 0.01 vs 0.41 ± 0.03 , $p = <0.001$), increased
277 Fulton Index (0.62 ± 0.05 vs. 0.31 ± 0.02 , $p = <0.001$), and increased RVSP (51.5 ± 5 vs. 22.4 ± 2

Exercising Blood Flow in Pulmonary Hypertension

278 mmHg, $p < 0.001$) compared with CON. Echocardiography revealed elevated RV thickness and
279 significant declines in cardiac function in MCT with reduced stroke volume, cardiac output,
280 cardiac index, pulmonary acceleration time, and a significantly increased pulmonary resistance
281 index and (Table 1).

	CON (n=16)	MCT (n=16)	p
RV thickness (m)	1.53 ± 0.1	2.27 ± 0.2	<0.001
Stroke Volume (μl)	264 ± 11	218 ± 13	0.011
Cardiac Output (mL/min)	86 ± 4	65 ± 5	0.001
Cardiac Index (mL·min ⁻¹ ·g ⁻¹)	0.22 ± 0.01	0.18 ± 0.01	0.008
PAAT (ms)	32 ± 1	26 ± 1	0.004
TPRi	43 ± 6	77 ± 16	0.02
HR	331 ± 7	308 ± 7	0.02

282 **Table 1:** Echocardiographic Measurements

283
284 Body weight, treadmill maximal aerobic capacity (VO₂max), and 12-hr volitional wheel
285 running distance was not different between groups pre MCT/vehicle injection ($p > 0.05$), however,
286 at final timepoint, body weight (335.3 ± 44.4 vs 400.3 ± 38.8 g, $p < 0.001$) and VO₂max ($53.1 \pm$
287 15.3 vs. 72.2 ± 8 ml/kg⁻¹/min⁻¹, $p < 0.001$) were significantly lower for the MCT (n=18) rats
288 compared to their CON (n=14) counterparts, and tended to be lower in wheel running distance
289 (498 ± 550 vs. 912 ± 638 m $p = 0.08$), consistent with the expected phenotype. Furthermore,
290 MCT demonstrated a significantly greater decline in VO₂max from pre to final timepoints when
291 compared to CON ($-13.1 \pm 1.9\%$ vs. $-38.9 \pm 7.8\%$, $p = 0.003$).

292 **Blood Flow**

293 Figure 3 demonstrates blood flow at rest and when expressed relative to power output
294 during exercise across all muscles for MCT and CON. At rest, no significant differences are seen
295 between groups, however, during exercise, skeletal muscle blood flow was significantly reduced
296 in MCT compared to CON ($p < 0.001$).

297
298
299
300
301
302
303
304
305
306
307
308
309
310
311
312
313
314
315
316
317

Metabolism

Blood lactate (Fig. 4) was not statistically different at rest in MCT compared to CON (p>0.05) however, during exercise, blood lactate was significantly elevated in MCT rats vs. CON (p=0.002).

Exercising blood lactate was inversely correlated to exercising blood flow in the EDL, **Fig 3.** Resting and exercising blood flow in MCT (n=7) vs. CON (n=8). At rest, no significant difference is seen between groups (p= 0.35). When expressed relative to power output during exercise, blood flow is significantly lower in MCT vs CON (p= <0.001). muscles sampled as well, including the gastrocnemius (r= -0.55, p= 0.06) and biceps femoris (r= -0.57, p= 0.05). When expressed as a compiled value for all skeletal muscles tested (average of eight muscles), a significant inverse association for blood flow with blood lactate during exercise was also observed (Fig 5D).

While there was no association for skeletal muscle blood flow at rest with any indicators of disease severity, there was a tendency for blood flow during exercise to be lower in animals with a more severe PH phenotype, such as with higher Fulton Index (r= -0.48, p=0.06) and lower cardiac output (r= 0.59, p=0.09).

Capillarization

There were no significant differences in capillarization between MCT and CON for either of the two skeletal muscles sampled, the predominantly type I muscle soleus, and the predominantly type II muscle EDL (Table 2, Fig 6).

Muscle	CON, n=8-9 (capillaries per myocyte)	MCT, n=9-13 (capillaries per myocyte)	p
EDL	0.96 ± 0.0	1.10 ± 0.1	0.12

Soleus	1.42 ± 0.1	1.45 ± 0.1	0.85
--------	------------	------------	------

Table 2. Capillary Density

318

319

Discussion

321 The purpose of this study was to investigate skeletal muscle blood flow at rest and during
322 exercise in a PH animal model. We determined that rats with MCT-induced PH and right heart
323 disease have reduced skeletal muscle blood flow during moderate intensity exercise when
324 compared to healthy controls, supporting previous work in both left heart failure (43-45) and
325 preliminary investigations into the hemodynamic responses to exercise in PAH patients (13, 46).
326 Additionally, we observed a significant relationship between reduced skeletal blood flow and
327 increased blood lactate during exercise. These findings add to the growing body of evidence
328 demonstrating the significance of muscle maladaptation in this disease.

329 The relative contributions of both central and peripheral dysfunction as they relate to
330 impaired performance in PAH continue to be debated. Undoubtedly, RV compromise attenuates
331 cardiac output response to exercise stress (16-21), however, peripheral manifestations of the
332 disease are now well established as additional contributors to observed performance decrements.
333 Previous work demonstrates that exercise intolerance can occur *independently* of cardiac
334 responses in PAH (13, 23), and improvements in physical function may occur without significant
335 central changes (47-49), supporting an important role of the periphery. We propose that reduced
336 skeletal muscle blood flow may pose a potentially important limitation to exercise tolerance as
337 well.

338 A prior report of impaired skeletal muscle blood flow in an MCT rat model of cardiac
339 disease included only resting measures and was limited to two muscles (42). To our knowledge,
340 this is the first study to *directly* measure skeletal muscle blood flow during exercise in an

341 experimental PAH model, and to demonstrate a robust deficiency across several muscle groups.
342 It is well established that at onset of exercise, blood flow and therefore oxygen delivery are
343 increased to meet the rising metabolic demands of skeletal muscle (45, 50), and there is a
344 growing body of evidence that this response is compromised in PAH. Most notably, it has been
345 demonstrated that circulatory abnormalities at the skeletal muscle level may contribute to a
346 reduced exercise performance. Evidence of microcirculatory loss (27), reduced oxygen
347 saturation/extraction (13, 31) and slower hyperemia responses (46) have all been suggested as
348 peripheral mechanisms restricting exercise tolerance in PAH. Our data obtained from directly
349 measured blood flow in a PAH model provides further evidence of circulatory dysfunction as a
350 peripheral contributor to disease sequelae.

351 Blood flow limitations during exercise have been characterized to a greater extent in left
352 heart failure, and although absolute values for blood flow are somewhat variable, the data tend to
353 support the findings in this study. Drexler, Faude, Höing and Just (43) demonstrated a
354 significant reduction to the gastrocnemius during maximal exercise in an infarct model of heart
355 failure. Later work in a similar model noted that rats more severely afflicted demonstrated the
356 most profound decrements in blood flow to exercising muscles (44). Interestingly, our data
357 closely mirrors this classic work as we describe higher resting blood flow in the soleus muscle in
358 comparison to the quadriceps and ankle flexors/extensors. While these early studies advanced a
359 novel insight into exercise intolerance in left heart failure, they have since been supported by
360 multiple investigations into exercises responses in the disease, comprehensively reviewed by
361 Poole, Hirai, Copp and Musch (45) and Hirai et al. (51). It has been shown that central
362 limitations in heart failure only partially explain a reduction in blood flow to working muscles in
363 LHF. While a reduced cardiac output may decrease the speed and magnitude of blood supply to

364 skeletal muscle at the onset of exercise, systemic vasoconstriction, vascular stiffness, endothelial
365 dysfunction, inflammatory markers and reduced NO bioavailability are all postulated as factors
366 culminating in compromised exercising blood flow in the disease (45).

367 In PAH, angiogenic deficiencies and microcirculatory loss have been implicated in
368 reduced exercise tolerance. Potus, Malenfant, Graydon, Mainguy, Tremblay, Breuils-Bonnet,
369 Ribeiro, Porlier, Maltais, Bonnet and Provencher (27) described a significant correlation between
370 downregulated angiogenic signaling in the quadriceps muscles of PAH patients and exercise
371 intolerance. In line with these findings, reduced capillarization was demonstrated in the RV of an
372 MCT rat model, secondary to downregulation of the HIF-1 pathway (52). This would indicate a
373 microcirculatory myopathy that extends to both the myocardium and peripheral muscle in PAH.
374 While reduced skeletal muscle capillarity could potentially provide an explanation for reduced
375 blood flow, we did not see a significant difference in capillary numbers between MCT and CON
376 rats. While we report slightly lower capillary to fiber ratios than previously described (53), we
377 note greater capillarization of the primarily Type I soleus compared to Type II EDL (54).
378 Regardless, in each muscle MCT did not induce rarefaction at the myocyte level. This contrasts
379 the aforementioned report of reduced capillarity in the RV after 6 weeks post MCT injection
380 (52). It is possible that more time is needed post-PH induction to see such changes at the skeletal
381 muscle level, or more significantly, that this model may not represent muscle abnormalities as
382 seen in PAH patients. With that said, our results would seem to contradict that of Potus,
383 Malenfant, Graydon, Mainguy, Tremblay, Breuils-Bonnet, Ribeiro, Porlier, Maltais, Bonnet and
384 Provencher (27) who showed that exercise intolerance was related to microcirculatory
385 dysfunction in patients, concomitant with a capillary loss in quadriceps muscle. However,
386 compelling evidence would seem to suggest that microcirculatory *function* rather than

Exercising Blood Flow in Pulmonary Hypertension

387 morphology better explains the control of blood flow to skeletal muscle during exercise (55).
388 Indeed, a recent study in an MCT rat has demonstrated muscle oxygen delivery is compromised
389 via reduced red blood cell flux, velocity and decreased capillary supporting flow in resting
390 skeletal muscle (56), further indicating the importance of hemodynamic control as a contributor
391 to muscle dysfunction in the disease. As such, future mechanistic investigations aimed at
392 explaining reduced muscle blood flow during exercise in this model should likely focus here.

393 There was a tendency for exercising blood flow to relate to disease measures, including
394 RV hypertrophy and cardiac output. It should be noted while cardiac output was measured at rest
395 via echocardiography, it may be the case that an exercise stimulus is required to elucidate the
396 connection between central and peripheral dysfunction in this model. Prior evidence has shown
397 that exercise stress (such as that carried out in an incremental exercise test) may be required to
398 identify physiological abnormalities that are central to disease progression, and may have an
399 important diagnostic role in the clinical setting (57, 58). Indeed, the presence of increased RV
400 pressures during exercise have been suggested as a precursor to resting PH (59), however, the
401 variable nature of responses to exercise in healthy individuals has made defining an ‘exercise
402 pulmonary hypertension’ an ongoing challenge (60). However, it is clear the integrated nature of
403 the exercise response can shed light on a host of clinically relevant factors, including the
404 metabolic, ventilatory and cardiovascular abnormalities present in the disease (4), and ultimately
405 determine the severity of disease and patient prognosis (61).

406 We have demonstrated a significant relationship between reduced skeletal muscle blood
407 flow and increased blood lactate accumulation during exercise in a PH rat model. Indeed, the
408 high lactates in combination with low muscle blood flows would suggest a severe heart failure
409 phenotype, further supported by the aforementioned decline in cardiac function and significant

410 RV hypertrophy in MCT rats. We suggest that our results may in fact underestimate the reduced
411 blood flow and lactate correlation, which is significantly strengthened when any potentially
412 errant rat data is removed from the analysis (Fig. 5). Nevertheless, a well-established hallmark of
413 the abnormal exercise response in PAH is a metabolic disturbance (12, 15, 28). Moreover, it has
414 previously been shown that high levels of serum lactate dehydrogenase indicative of metabolic
415 abnormality independently predicts functional status in PAH patients (62). Lactate and hydrogen
416 ions accumulate in the blood as a result of several interrelated mechanisms, including a reliance
417 on non-aerobic glycolysis, conversion of pyruvate to lactate and reduced systemic clearance via
418 lactate oxidation contributing to the onset of fatigue (comprehensively reviewed by Poole et al.
419 (63). Previous work in PAH has shown an early accumulation of lactate relative to exercise
420 intensity (4), indicating an ineffective switch from aerobic to anaerobic means of ATP
421 production. Several mechanisms may explain this phenomenon in PAH, including blunted
422 cardiac response to exercise (7, 8, 16, 26) and muscle adaptations that compromise oxidative
423 metabolism (10-12, 28, 29). Our results suggest an association between cardiovascular
424 maladaptation's driven by disease and a metabolic disturbance that may limit exercise capacity
425 in PAH. Further investigation should therefore interrogate the role of mitochondrial dysfunction
426 in exercise limitation for this population.

427 We note limitations in this study. While the monocrotaline model has been widely used
428 in pulmonary hypertension research for decades, the mechanisms by which pulmonary pressure
429 and hemodynamic abnormalities arise may not adequately replicate human disease. Additionally,
430 there is compelling evidence that multiple organ systems are impacted by MCT administration.
431 Some 50 years ago Roth et al. (64) noted injuries to the liver, kidneys and lungs of rats exposed to
432 MCT in drinking water. More recently, this has been supported by a number of studies reporting

433 vascular changes in the lungs of MCT treated rats, leading to the idea of an “MCT-syndrome”
434 proposed by Gomez-Arroyo et al. (65). As such, we are unable to definitively state that the
435 skeletal muscle changes are solely a result of PH modeling without a more direct effect of MCT
436 on skeletal muscle morphology and function. Indeed, we recommend the further study of MCT
437 on skeletal muscle tissue more broadly, as undoubtedly this model will continue to be
438 implemented in PH animal studies. Crucially, MCT does not reliably induce a PH phenotype in
439 the female rat (32). As such, future investigations should assess alternative models, with the
440 inclusion female animals highly encouraged. Although our results demonstrate blood flow was
441 lower in MCT animals relative to power output during exercise, this difference may be partially
442 due to different absolute exercise intensities between groups. Finally, while we have
443 demonstrated reduced skeletal muscle blood flow in an MCT rat, the mechanisms behind this
444 deficit remain to be elucidated. We have shown that capillary rarefaction in this model is likely
445 not a determining factor, hence future work should focus on vascular function as it related to
446 muscle perfusion.

447 In conclusion, we have shown that in a PAH animal model, skeletal blood flow is
448 significantly reduced during moderate intensity exercise. These findings can be linked to
449 previous work in this area, most notably that tissue oxygen supply and extraction are reduced in
450 patients with PAH. We further observed an association between exercising blood flow and
451 lactate accumulation, suggesting that both central and peripheral factors may lead to metabolic
452 disturbance and exercise limitation in the disease. These findings lend weight to the developing
453 idea that pharmacologic, exercise, and/or nutritional strategies specifically aimed at combating
454 skeletal muscle dysfunction in PAH are warranted, and may ultimately provide a novel adjuvant
455 treatment method.

456 **Grants**

457 This work was supported by the National Heart, Lung, and Blood Institute (NHLBI) of the
458 National Institutes of Health, Grant number R15 HL121661 (to M. B. Brown).

459

460 **References**

- 461 1. **Galie N, Palazzini M, and Manes A.** Pulmonary arterial hypertension: from the
462 kingdom of the near-dead to multiple clinical trial meta-analyses. *Eur Heart J* 31: 2080-2086,
463 2010.
- 464 2. **Boucly A, Weatherald J, Savale L, Jaïs X, Cottin V, Prevoit G, Picard F, de Groot
465 P, Jevnikar M, Bergot E, Chaouat A, Chabanne C, Bourdin A, Parent F, Montani D,
466 Simonneau G, Humbert M, and Sitbon O.** Risk assessment, prognosis and guideline
467 implementation in pulmonary arterial hypertension. *Eur Respir J* 50: 2017.
- 468 3. **Babu AS, Arena R, Myers J, Padmakumar R, Maiya AG, Cahalin LP, Waxman AB,
469 and Lavie CJ.** Exercise intolerance in pulmonary hypertension: mechanism, evaluation and
470 clinical implications. *Expert Rev Respir Med* 1-12, 2016.
- 471 4. **Neder JA, Ramos RP, Ota-Arakaki JS, Hirai DM, D'Arsigny CL, and O'Donnell D.**
472 Exercise intolerance in pulmonary arterial hypertension. The role of cardiopulmonary exercise
473 testing. *Ann Am Thorac Soc* 12: 604-612, 2015.
- 474 5. **Tran DL, Lau EMT, Celermajor DS, Davis GM, and Cordina R.** Pathophysiology of
475 exercise intolerance in pulmonary arterial hypertension. *Respirology* 23: 148-159, 2018.
- 476 6. **Arena R, Lavie CJ, Milani RV, Myers J, and Guazzi M.** Cardiopulmonary exercise
477 testing in patients with pulmonary arterial hypertension: an evidence-based review. *J Heart Lung*
478 *Transplant* 29: 159-173, 2010.
- 479 7. **Sun XG, Hansen JE, Oudiz RJ, and Wasserman K.** Exercise pathophysiology in
480 patients with primary pulmonary hypertension. *Circulation* 104: 429-435, 2001.
- 481 8. **Waxman AB.** Exercise physiology and pulmonary arterial hypertension. *Prog*
482 *Cardiovasc Dis* 55: 172-179, 2012.
- 483 9. **Deboeck G, Niset G, Lamotte M, Vachiéry JL, and Naeije R.** Exercise testing in
484 pulmonary arterial hypertension and in chronic heart failure. *Eur Respir J* 23: 747-751, 2004.
- 485 10. **Batt J, Ahmed SS, Correa J, Bain A, and Granton J.** Skeletal muscle dysfunction in
486 idiopathic pulmonary arterial hypertension. *Am J Respir Cell Mol Biol* 50: 74-86, 2014.
- 487 11. **de Man FS, van Hees HW, Handoko ML, Niessen HW, Schaliij I, Humbert M,
488 Dorfmueller P, Mercier O, Bogaard HJ, Postmus PE, Westerhof N, Stienen GJ, van der
489 Laarse WJ, Vonk-Noordegraaf A, and Ottenheijm CA.** Diaphragm muscle fiber weakness in
490 pulmonary hypertension. *Am J Respir Crit Care Med* 183: 1411-1418, 2011.
- 491 12. **Mainguy V, Maltais F, Saey D, Gagnon P, Martel S, Simon M, and Provencher S.**
492 Peripheral muscle dysfunction in idiopathic pulmonary arterial hypertension. *Thorax* 65: 113-
493 117, 2010.
- 494 13. **Malenfant S, Potus F, Mainguy V, Leblanc E, Malenfant M, Ribeiro F, Saey D,
495 Maltais F, Bonnet S, and Provencher S.** Impaired Skeletal Muscle Oxygenation and Exercise
496 Tolerance in Pulmonary Hypertension. *Med Sci Sports Exerc* 47: 2273-2282, 2015.

- 497 14. **D'Alonzo GE, Gianotti LA, Pohil RL, Reagle RR, DuRee SL, Fuentes F, and**
498 **Dantzker DR.** Comparison of progressive exercise performance of normal subjects and patients
499 with primary pulmonary hypertension. *Chest* 92: 57-62, 1987.
- 500 15. **Malenfant S, Lebret M, Breton-Gagnon É, Potus F, Paulin R, Bonnet S, and**
501 **Provencher S.** Exercise intolerance in pulmonary arterial hypertension: insight into central and
502 peripheral pathophysiological mechanisms. *Eur Respir Rev* 30: 2021.
- 503 16. **Holverda S, Gan CT, Marcus JT, Postmus PE, Boonstra A, and Vonk-Noordegraaf**
504 **A.** Impaired stroke volume response to exercise in pulmonary arterial hypertension. *J Am Coll*
505 *Cardiol* 47: 1732-1733, 2006.
- 506 17. **Provencher S, Chemla D, Herve P, Sitbon O, Humbert M, and Simonneau G.** Heart
507 rate responses during the 6-minute walk test in pulmonary arterial hypertension. *Eur Respir J* 27:
508 114-120, 2006.
- 509 18. **Badagliacca R, Papa S, Valli G, Pezzuto B, Poscia R, Reali M, Manzi G, Giannetta**
510 **E, Berardi D, Sciomer S, Palange P, Fedele F, Naeije R, and Vizza CD.** Right ventricular
511 dyssynchrony and exercise capacity in idiopathic pulmonary arterial hypertension. *Eur Respir J*
512 49: 2017.
- 513 19. **Hill AC, Maxey DM, Rosenthal DN, Siehr SL, Hollander SA, Feinstein JA, and**
514 **Dubin AM.** Electrical and mechanical dyssynchrony in pediatric pulmonary hypertension. *J*
515 *Heart Lung Transplant* 31: 825-830, 2012.
- 516 20. **Marcus JT, Gan CT, Zwanenburg JJ, Boonstra A, Allaart CP, Gotte MJ, and**
517 **Vonk-Noordegraaf A.** Interventricular mechanical asynchrony in pulmonary arterial
518 hypertension: left-to-right delay in peak shortening is related to right ventricular overload and
519 left ventricular underfilling. *J Am Coll Cardiol* 51: 750-757, 2008.
- 520 21. **Spruijt OA, de Man FS, Groepenhoff H, Oosterveer F, Westerhof N, Vonk-**
521 **Noordegraaf A, and Bogaard HJ.** The effects of exercise on right ventricular contractility and
522 right ventricular-arterial coupling in pulmonary hypertension. *Am J Respir Crit Care Med* 191:
523 1050-1057, 2015.
- 524 22. **Aslan GK, Akinci B, Yeldan I, and Okumus G.** Respiratory muscle strength in patients
525 with pulmonary hypertension: The relationship with exercise capacity, physical activity level,
526 and quality of life. *The clinical respiratory journal* 12: 699-705, 2018.
- 527 23. **Breda AP, Pereira de Albuquerque AL, Jardim C, Morinaga LK, Suesada MM,**
528 **Fernandes CJ, Dias B, Lourenco RB, Salge JM, and Souza R.** Skeletal muscle abnormalities
529 in pulmonary arterial hypertension. *PloS one* 9: e114101, 2014.
- 530 24. **Saglam M, Vardar-Yagli N, Calik-Kutukcu E, Arikan H, Savci S, Inal-Ince D,**
531 **Akdogan A, and Tokgozoglul L.** Functional exercise capacity, physical activity, and respiratory
532 and peripheral muscle strength in pulmonary hypertension according to disease severity. *Journal*
533 *of physical therapy science* 27: 1309-1312, 2015.
- 534 25. **Bauer R, Dehnert C, Schoene P, Filusch A, Bartsch P, Borst MM, Katus HA, and**
535 **Meyer FJ.** Skeletal muscle dysfunction in patients with idiopathic pulmonary arterial
536 hypertension. *Respiratory medicine* 101: 2366-2369, 2007.
- 537 26. **Manders E, Rain S, Bogaard HJ, Handoko ML, Stienen GJ, Vonk-Noordegraaf A,**
538 **Ottenheijm CA, and de Man FS.** The striated muscles in pulmonary arterial hypertension:
539 adaptations beyond the right ventricle. *Eur Respir J* 46: 832-842, 2015.
- 540 27. **Potus F, Malenfant S, Graydon C, Mainguy V, Tremblay E, Breuils-Bonnet S,**
541 **Ribeiro F, Porlier A, Maltais F, Bonnet S, and Provencher S.** Impaired angiogenesis and

- 542 peripheral muscle microcirculation loss contribute to exercise intolerance in pulmonary arterial
543 hypertension. *Am J Respir Crit Care Med* 190: 318-328, 2014.
- 544 28. **Malenfant S, Potus F, Fournier F, Breuils-Bonnet S, Pflieger A, Bourassa S,**
545 **Tremblay E, Nehme B, Droit A, Bonnet S, and Provencher S.** Skeletal muscle proteomic
546 signature and metabolic impairment in pulmonary hypertension. *J Mol Med (Berl)* 93: 573-584,
547 2015.
- 548 29. **Brown MB, Chingombe TJ, Zinn AB, Reddy JG, Novack RA, Cooney SA, Fisher**
549 **AJ, Presson RG, Lahm T, and Petrache I.** Novel assessment of haemodynamic kinetics with
550 acute exercise in a rat model of pulmonary arterial hypertension. *Exp Physiol* 100: 742-754,
551 2015.
- 552 30. **Enache I, Charles AL, Bouitbir J, Favret F, Zoll J, Metzger D, Oswald-Mammosser**
553 **M, Geny B, and Charloux A.** Skeletal muscle mitochondrial dysfunction precedes right
554 ventricular impairment in experimental pulmonary hypertension. *Mol Cell Biochem* 373: 161-
555 170, 2013.
- 556 31. **Tolle J, Waxman A, and Systrom D.** Impaired systemic oxygen extraction at maximum
557 exercise in pulmonary hypertension. *Med Sci Sports Exerc* 40: 3-8, 2008.
- 558 32. **Bal E, Ilgin S, Atli O, Ergun B, and Sirmagul B.** The effects of gender difference on
559 monocrotaline-induced pulmonary hypertension in rats. *Hum Exp Toxicol* 32: 766-774, 2013.
- 560 33. **Mark Lafronconi W, and Huxtable RJ.** Hepatic metabolism and pulmonary toxicity of
561 monocrotaline using isolated perfused liver and lung. *Biochemical Pharmacology* 33: 2479-
562 2484, 1984.
- 563 34. **Kasahara Y, Kiyatake K, Tatsumi K, Sugito K, Kakusaka I, Yamagata S-i, Ohmori**
564 **S, Kitada M, and Kuriyama T.** Bioactivation of Monocrotaline by P-450 3A in Rat Liver.
565 *Journal of cardiovascular pharmacology* 30: 1997.
- 566 35. **Kemi OJ, Loennechen JP, Wisloff U, and Ellingsen O.** Intensity-controlled treadmill
567 running in mice: cardiac and skeletal muscle hypertrophy. *Journal of applied physiology*
568 *(Bethesda, Md : 1985)* 93: 1301-1309, 2002.
- 569 36. **Brown MB, Neves E, Long G, Graber J, Gladish B, Wiseman A, Owens M, Fisher**
570 **AJ, Presson RG, Petrache I, Kline J, and Lahm T.** High-intensity interval training, but not
571 continuous training, reverses right ventricular hypertrophy and dysfunction in a rat model of
572 pulmonary hypertension. *American journal of physiology Regulatory, integrative and*
573 *comparative physiology* 312: R197-r210, 2017.
- 574 37. **Ishise S, Pegram BL, Yamamoto J, Kitamura Y, and Frohlich ED.** Reference sample
575 microsphere method: cardiac output and blood flows in conscious rat. *Am J Physiol* 239: H443-
576 h449, 1980.
- 577 38. **Glenny RW, Bernard S, and Brinkley M.** Validation of fluorescent-labeled
578 microspheres for measurement of regional organ perfusion. *Journal of applied physiology*
579 *(Bethesda, Md : 1985)* 74: 2585-2597, 1993.
- 580 39. **Armstrong RB, Hayes DA, and Delp MD.** Blood flow distribution in rat muscles during
581 preexercise anticipatory response. *Journal of Applied Physiology* 67: 1855-1861, 1989.
- 582 40. **Lu SS, Lau CP, Tung YF, Huang SW, Chen YH, Shih HC, Tsai SC, Lu CC, Wang**
583 **SW, Chen JJ, Chien EJ, Chien CH, and Wang PS.** Lactate stimulates progesterone secretion
584 via an increase in cAMP production in exercised female rats. *The American journal of*
585 *physiology* 271: E910-915, 1996.

- 586 41. **Kato M, Kurakane S, Nishina A, Park J, and Chang H.** The blood lactate increase in
587 high intensity exercise is depressed by *Acanthopanax sieboldianus*. *Nutrients* 5: 4134-4144,
588 2013.
- 589 42. **Vescovo G, Ceconi C, Bernocchi P, Ferrari R, Carraro U, Ambrosio GB, and Libera**
590 **LD.** Skeletal muscle myosin heavy chain expression in rats with monocrotaline-induced cardiac
591 hypertrophy and failure. Relation to blood flow and degree of muscle atrophy. *Cardiovasc Res*
592 39: 233-241, 1998.
- 593 43. **Drexler H, Faude F, Höing S, and Just H.** Blood flow distribution within skeletal
594 muscle during exercise in the presence of chronic heart failure: effect of milrinone. *Circulation*
595 76: 1344-1352, 1987.
- 596 44. **Musch TI, and Terrell JA.** Skeletal muscle blood flow abnormalities in rats with a
597 chronic myocardial infarction: rest and exercise. *American Journal of Physiology-Heart and*
598 *Circulatory Physiology* 262: H411-H419, 1992.
- 599 45. **Poole DC, Hirai DM, Copp SW, and Musch TI.** Muscle oxygen transport and
600 utilization in heart failure: implications for exercise (in)tolerance. *Am J Physiol Heart Circ*
601 *Physiol* 302: H1050-1063, 2012.
- 602 46. **Dimopoulos S, Tzanis G, Manetos C, Tasoulis A, Mpouchla A, Tseliou E, Vasileiadis**
603 **I, Diakos N, Terrovitis J, and Nanas S.** Peripheral Muscle Microcirculatory Alterations in
604 Patients With Pulmonary Arterial Hypertension: A Pilot Study. *Respiratory Care* 58: 2134-2141,
605 2013.
- 606 47. **Chan L, Chin LMK, Kennedy M, Woolstenhulme JG, Nathan SD, Weinstein AA,**
607 **Connors G, Weir NA, Drinkard B, Lamberti J, and Keyser RE.** Benefits of intensive
608 treadmill exercise training on cardiorespiratory function and quality of life in patients with
609 pulmonary hypertension. *Chest* 143: 333-343, 2013.
- 610 48. **Fox BD, Kassirer M, Weiss I, Raviv Y, Peled N, Shitrit D, and Kramer MR.**
611 Ambulatory rehabilitation improves exercise capacity in patients with pulmonary hypertension. *J*
612 *Card Fail* 17: 196-200, 2011.
- 613 49. **Mereles D, Ehlken N, Kreuscher S, Ghofrani S, Hoepfer MM, Halank M, Meyer FJ,**
614 **Karger G, Buss J, Juenger J, Holzapfel N, Opitz C, Winkler J, Herth FF, Wilkens H, Katus**
615 **HA, Olschewski H, and Grunig E.** Exercise and respiratory training improve exercise capacity
616 and quality of life in patients with severe chronic pulmonary hypertension. *Circulation* 114:
617 1482-1489, 2006.
- 618 50. **Sarelius I, and Pohl U.** Control of muscle blood flow during exercise: local factors and
619 integrative mechanisms. *Acta Physiol (Oxf)* 199: 349-365, 2010.
- 620 51. **Hirai DM, Musch TI, and Poole DC.** Exercise training in chronic heart failure:
621 improving skeletal muscle O₂ transport and utilization. *Am J Physiol Heart Circ Physiol* 309:
622 H1419-1439, 2015.
- 623 52. **Sutendra G, Dromparis P, Paulin R, Zervopoulos S, Haromy A, Nagendran J, and**
624 **Michelakis ED.** A metabolic remodeling in right ventricular hypertrophy is associated with
625 decreased angiogenesis and a transition from a compensated to a decompensated state in
626 pulmonary hypertension. *J Mol Med (Berl)* 91: 1315-1327, 2013.
- 627 53. **Poole DC, Mathieu-Costello O, and West JB.** Capillary tortuosity in rat soleus muscle
628 is not affected by endurance training. *Am J Physiol* 256: H1110-1116, 1989.
- 629 54. **Armstrong RB, and Phelps RO.** Muscle fiber type composition of the rat hindlimb. *Am*
630 *J Anat* 171: 259-272, 1984.

- 631 55. **Laughlin MH, Davis MJ, Secher NH, van Lieshout JJ, Arce-Esquivel AA, Simmons**
632 **GH, Bender SB, Padilla J, Bache RJ, Merkus D, and Duncker DJ.** Peripheral Circulation. In:
633 *Comprehensive Physiology*. 321-447.
- 634 56. **Schulze KM, Weber RE, Horn AG, Colburn TD, Ade CJ, Poole DC, and Musch TI.**
635 Effects of pulmonary hypertension on microcirculatory hemodynamics in rat skeletal muscle.
636 *Microvascular Research* 141: 104334, 2022.
- 637 57. **Hsu S, Houston BA, Tampakakis E, Bacher AC, Rhodes PS, Mathai SC, Damico**
638 **RL, Kolb TM, Hummers LK, Shah AA, McMahan Z, Corona-Villalobos CP, Zimmerman**
639 **SL, Wigley FM, Hassoun PM, Kass DA, and Tedford RJ.** Right Ventricular Functional
640 Reserve in Pulmonary Arterial Hypertension. *Circulation* 133: 2413-2422, 2016.
- 641 58. **Farina S, Correale M, Bruno N, Paolillo S, Salvioni E, Badagliacca R, and Agostoni**
642 **P.** The role of cardiopulmonary exercise tests in pulmonary arterial hypertension. *European*
643 *Respiratory Review* 27: 170134, 2018.
- 644 59. **Medarov BI, Jogani S, Sun J, and Judson MA.** Readdressing the entity of exercise
645 pulmonary arterial hypertension. *Respiratory medicine* 124: 65-71, 2017.
- 646 60. **Simonneau G, Montani D, Celermajer DS, Denton CP, Gatzoulis MA, Krowka M,**
647 **Williams PG, and Souza R.** Haemodynamic definitions and updated clinical classification of
648 pulmonary hypertension. *European Respiratory Journal* 53: 1801913, 2019.
- 649 61. **Paolillo S, Farina S, Bussotti M, Iorio A, PerroneFilardi P, Piepolil MF, and**
650 **Agostoni P.** Exercise testing in the clinical management of patients affected by pulmonary
651 arterial hypertension. *Eur J Prev Cardiol* 19: 960-971, 2012.
- 652 62. **Hu EC, He JG, Liu ZH, Ni XH, Zheng YG, Gu Q, Zhao ZH, and Xiong CM.** High
653 levels of serum lactate dehydrogenase correlate with the severity and mortality of idiopathic
654 pulmonary arterial hypertension. *Exp Ther Med* 9: 2109-2113, 2015.
- 655 63. **Poole DC, Rossiter HB, Brooks GA, and Gladden LB.** The anaerobic threshold: 50+
656 years of controversy. *J Physiol* 599: 737-767, 2021.
- 657 64. **Roth RA, Dotzlaf LA, Baranyi B, Kuo CH, and Hook JB.** Effect of monocrotaline
658 ingestion on liver, kidney, and lung of rats. *Toxicology and Applied Pharmacology* 60: 193-203,
659 1981.
- 660 65. **Gomez-Arroyo JG, Farkas L, Alhussaini AA, Farkas D, Kraskauskas D, Voelkel**
661 **NF, and Bogaard HJ.** The monocrotaline model of pulmonary hypertension in perspective. *Am*
662 *J Physiol Lung Cell Mol Physiol* 302: L363-369, 2012.
- 663

664 **Figures**

665
666 **Fig 1.** Study Protocol

668 **Fig 2: A-C**

669 PH phenotype as evidenced by increased RV weight (0.22 ± 0.01 vs 0.41 ± 0.03), increased
670 Fulton Index (0.62 ± 0.05 vs. 0.31 ± 0.02), and increased RVSP (51.5 ± 5 vs. 22.4 ± 2 mmHg) in
671 MCT (n=12-13) compared with CON (n=11). *p = <0.05, **p = <0.001. RV: Right Ventricle;
672 RVSP: Right Ventricular Systolic Pressure

673

Exercising Blood Flow in Pulmonary Hypertension

674 **Fig 3:** Resting and exercising blood flow in MCT (n=7) vs. CON (n=8). At rest, no significant
675 difference is seen between groups ($p= 0.35$). When expressed relative to power output during
676 exercise, blood flow is significantly lower in MCT vs CON ($p= <0.001$).

677

678 **Fig 4:**

679 **Fig. 4** Evidence of altered metabolism during exercise via increased blood lactate in MCT
680 (n=23) vs. CON (n=16). * $p= <0.05$

681

682 **Fig 5:**

683 **Fig 5:** Exercising blood lactate was inversely correlated to exercising blood flow in the EDL,
684 tibialis anterior, and soleus, and a significant inverse association for blood flow with blood
685 lactate during exercise was also observed when blood flow is expressed as a compiled value for
686 all skeletal muscles (n-12). EDL: Extensor digitorum longus; TA: Tibialis anterior; SL, Soleus.

687

688 **Fig 6:**

689 Representative images of immunofluorescent staining of muscle tissue imaged at 10x
690 magnification. Capillaries (yellow, as overlay of green and red), myocyte membrane
691 (glycoproteins, green), vasculature (lectin, red), nuclei (DAPI, blue) in soleus muscle sections.

692

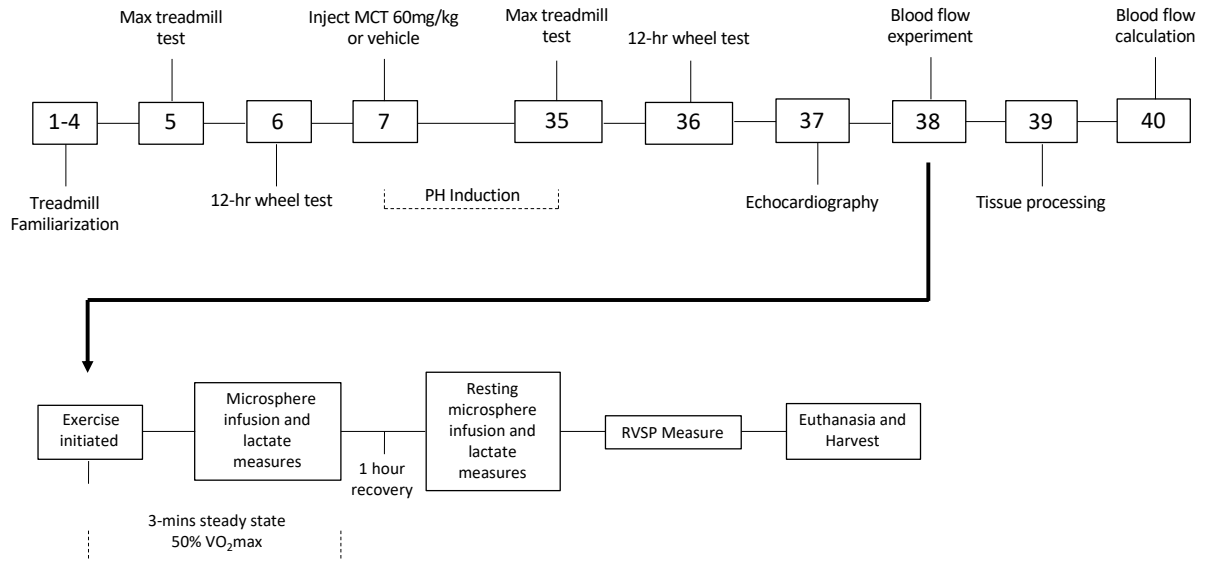


Figure 1

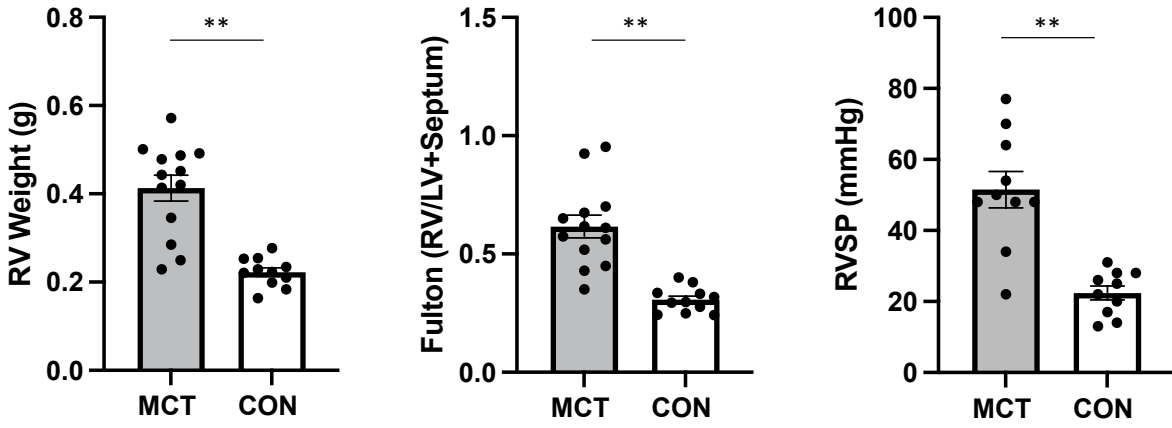


Figure 2

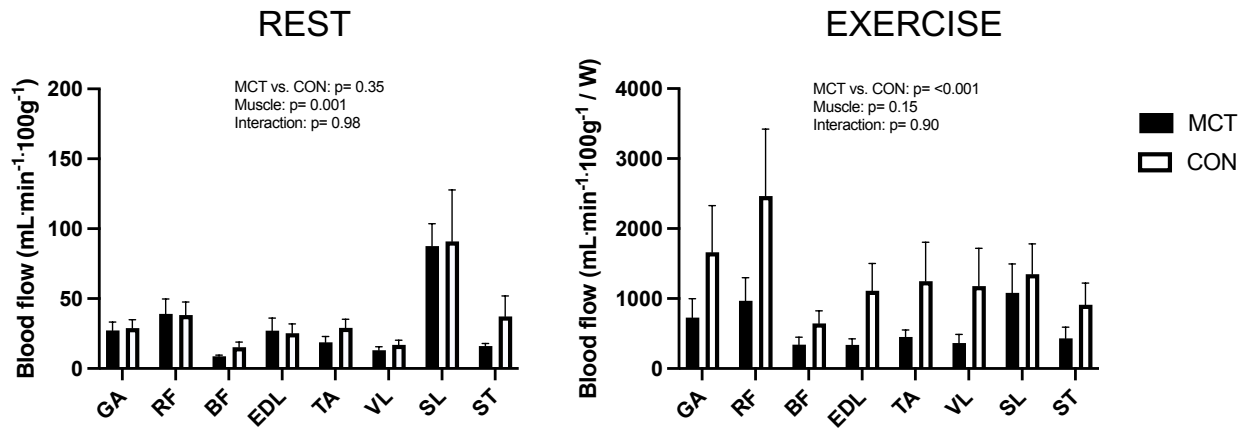


Figure 3

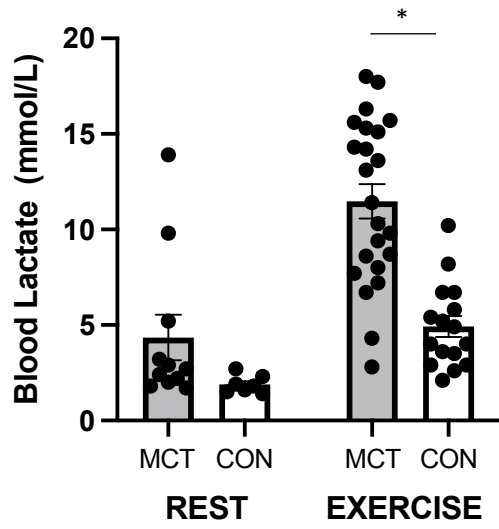


Figure 4

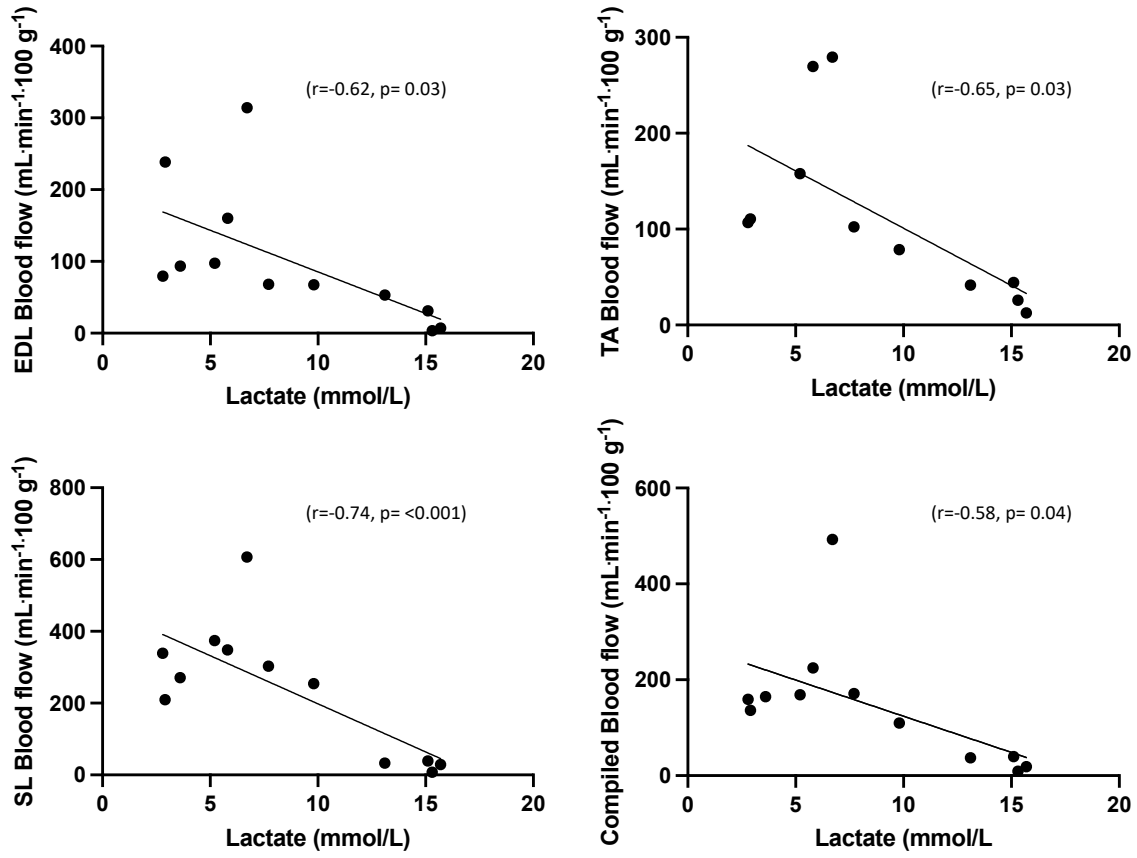


Figure 5

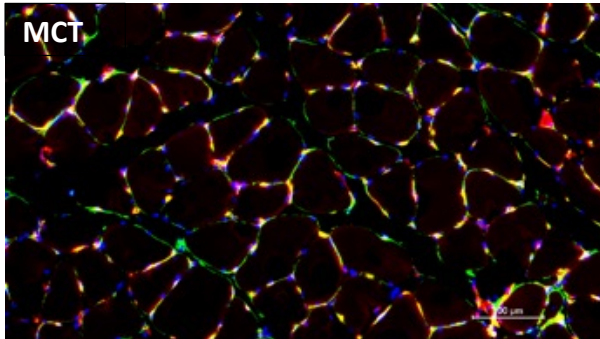
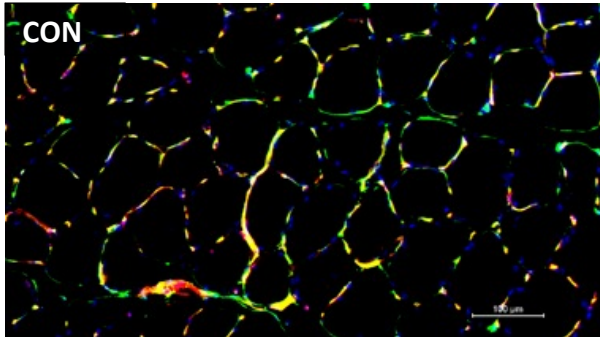


Figure 6